SIMS Proceedings Papers

SURFACE and INTERFACE ANALYSIS

Received: 11 September 2009 Revised: 19 April 2010 Accepted: 19 April 2010 Published online in Wiley Online Library: 22 June 2010

(wileyonlinelibrary.com) DOI 10.1002/sia.3592

Photon emission from massive projectile impacts on solids

F. A. Fernandez-Lima,[a] V. T. Pinnick,[a] S. Della-Negra[b] and E. A. Schweikert[a]*

First evidence of photon emission from individual impacts of massive gold projectiles on solids for a number of projectile-target combinations is reported. Photon emission from individual impacts of massive Au_n^{+q} ($1 \leq n \leq 400$; $q = 1–4$) projectiles with impact energies in the range of 28–136 keV occurs in less than 10 ns after the projectile impact. Experimental observations show an increase in the photon yield from individual impacts with the projectile size and velocity. Concurrently with the photon emission, electron emission from the impact area has been observed below the kinetic emission threshold and under unlikely conditions for potential electron emission. We interpret the puzzling electron emission and correlated luminescence observation as evidence of the electronic excitation resulting from the high-energy density deposited by massive cluster projectiles during the impact.

Keywords: massive cluster keV projectiles; SIMS; photon emission; electron emission

Introduction

Photon emission from surfaces exposed to ion bombardment is well documented.[1,2] In keV atomic ion beam bombardment, light emission can originate from sputtered atoms, back-scattered primary ions, or from the target.[3–5] Photon emission can still be detected when the bombardment regime is reduced to temporally and spatially discrete impacts of individual keV atomic and polyatomic ions.[6,7] In this case, where beam effects are absent, photon emission from ionic targets could be assigned to electronic excitation inside the solid. Indeed, under single impact conditions, the processes leading to observable photon emission can occur before ion emission (10^{-13} vs 10^{-12}, respectively), thus, inspection of the photon emission can provide information on the underlying physical processes that govern the projectile-target interaction.[8]

Light flashes from single impacts of micrometer-size particles in the hydrodynamic regime have been observed in interstellar mediums.[9] Experimental studies and MD simulations indicate that massive keV projectiles are implanted in the solid via hydrodynamic penetration.[10,11] In the present paper, we present the first experimental observation of photon emission in hydrodynamic penetration with nm-size projectiles, and compare the observations with those observed from atomic and small polyatomic projectiles. Concurrently with the luminescence process, the electron and negative secondary ion emission from the projectile impact site is determined.

Experimental

Details on the Au_n^{+q} ($1 \leq n \leq 400$; $q = 1–4$) primary ion production and selection can be found elsewhere.[12] Briefly, a liquid metal ion source (LMIS) generates a broad distribution of gold projectiles, which are further separated using a Wien filter to guarantee the primary ion of interest (Fig. 1). The single impact regime is achieved by pulsing the primary ion beam at ~5–10 kHz through a series of primary ion beam collimators. Photon, electron and secondary ion (SI) emissions are collected per projectile impact. Photon emission is detected using a photon-counting photo multiplier (PMT, R4220P model from Hamamatsu Photonics), with an active window from 185 to 710 nm, a maximum 22% detection efficiency at 410 nm, and positioned behind the target (solid angle of 0.8π sr). Secondary electrons are accelerated and then deviated using a magnetic field towards an offline MCP detector, which are used as starts for the SI ToF. The ToF stop signals of the SIs are collected using a MCP coupled to a multianode detector positioned ~100 cm from the target surface, and are stored in an eight-channel time-to-digital converter (TDC). The photon signal from individual impacts is time delayed and stored in one of the eight TDC channels. Cesium Iodide, Acid Blue 25 (AB25), Sulforodhamine B (SRB), and Fluorescein isothiocyanate (FITC) samples were obtained from Sigma Aldrich (St. Louis, MO) and used as received. Surface target homogeneity was achieved using either electrospray or vapor deposition techniques; the sample thickness was kept larger than the projectile range. All samples were deposited onto a 70–100 Ω/sq indium tin oxide-coated glass (ITO/glass) substrate from Sigma Aldrich (St. Loius, MO). Relative photon yields dependence on the projectile size and energy are reported; no photon emission was observed upon the bombardment of the bare ITO substrate.

Results and Discussion

Typical time-resolved spectra of photon emission for monoatomic (Au_1^{+}), polyatomic (Au_3^{+}) and massive (Au_{200}^{+4} and Au_{400}^{+4}) gold projectiles are presented in Fig. 2. Significant differences can be observed in the photon emission distribution as the projectile size

* *Correspondence to: E. A. Schweikert, Department of Chemistry, Texas A&M University, College Station, TX, 77843, USA. E-mail: schweikert@chem.tamu.edu*

a *Department of Chemistry, Texas A&M University, College Station, TX, 77843, USA*

b *Institut de Physique Nucléaire, B.P. No. 1, F-91406 Orsay Cedex, France*

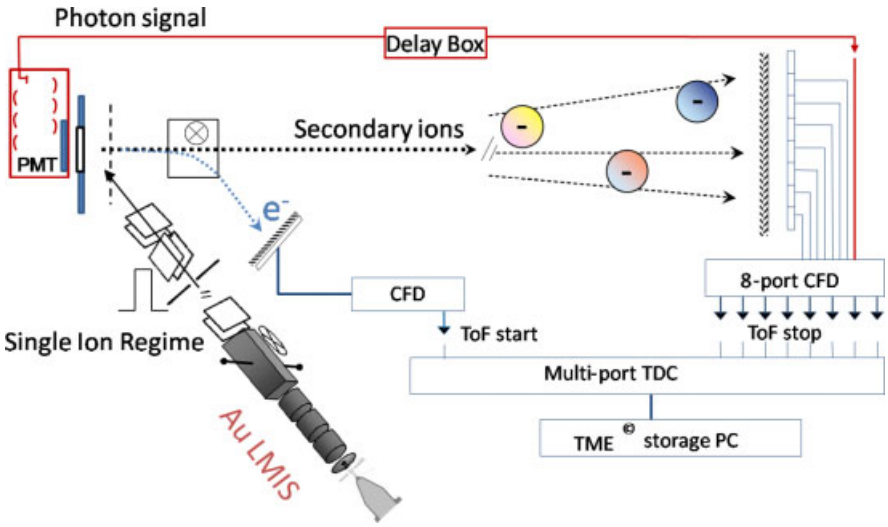

Figure 1. Schematics of the experimental setup used for the simultaneous observation of photon, electron and secondary ion emission from individual Au projectile impacts.

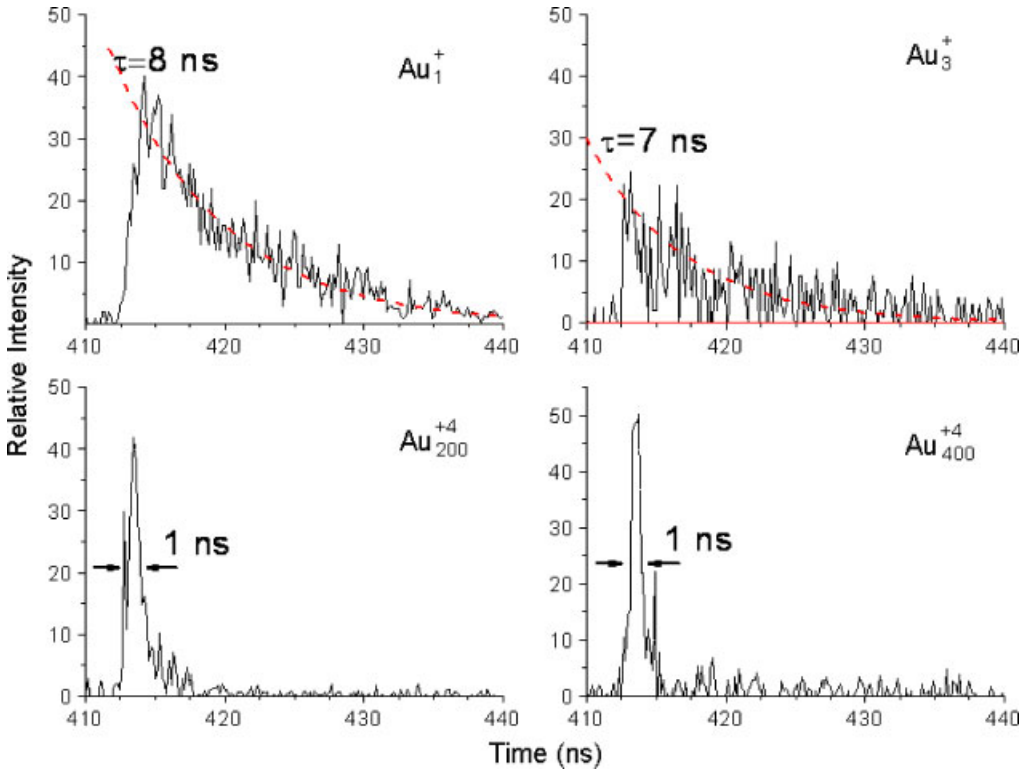

Figure 2. Photon time emission from a CsI/ITO target bombarded with individual gold projectiles (34 qkeV) as a function of the projectile size. Photon signals were time delayed and recorded relative to the electron emission signal (schematics of the setup in Fig. 1).

increases from monoatomic to polyatomic to massive cluster. For example, the CsI/ITO time-resolved photon spectra produced by monoatomic and polyatomic gold projectiles can be characterized by a long tail distribution with a lifetime of $\tau = 7-8$ ns (considering that $I(t) = Io \times \exp(-t/\tau)$). Similar exponential distributions have been previously observed under the bombardment of CsI targets with individual monoatomic projectiles (e.g. 45 keV H^- and I^- ions).[6] However, the CsI/ITO time-resolved spectra produced by massive gold projectiles ($Au_{100}{}^{+4}$–$Au_{400}{}^{+4}$) presents a distinctly distribution: it can be characterized by a narrow Gaussian distribution (FWHM ~1 ns) and no exponential decay is observed. Similar trends were observed for organic samples.

Pure CsI is used at room temperature as a fast scintillator (decay time <10 ns) in electromagnetic calorimeters at high counting rates[13,14] and in nuclear physics for 4π charged product detection array.[15] The studies of the light emission of this crystal show that CsI (pure) presents after electronic excitation a photon electron emission with a short decay time of ~16 ns (10–30 ns) which normally represents at least 70% of the light emission. It is a UV emission, the wavelength is around 310–320 nm and corresponds

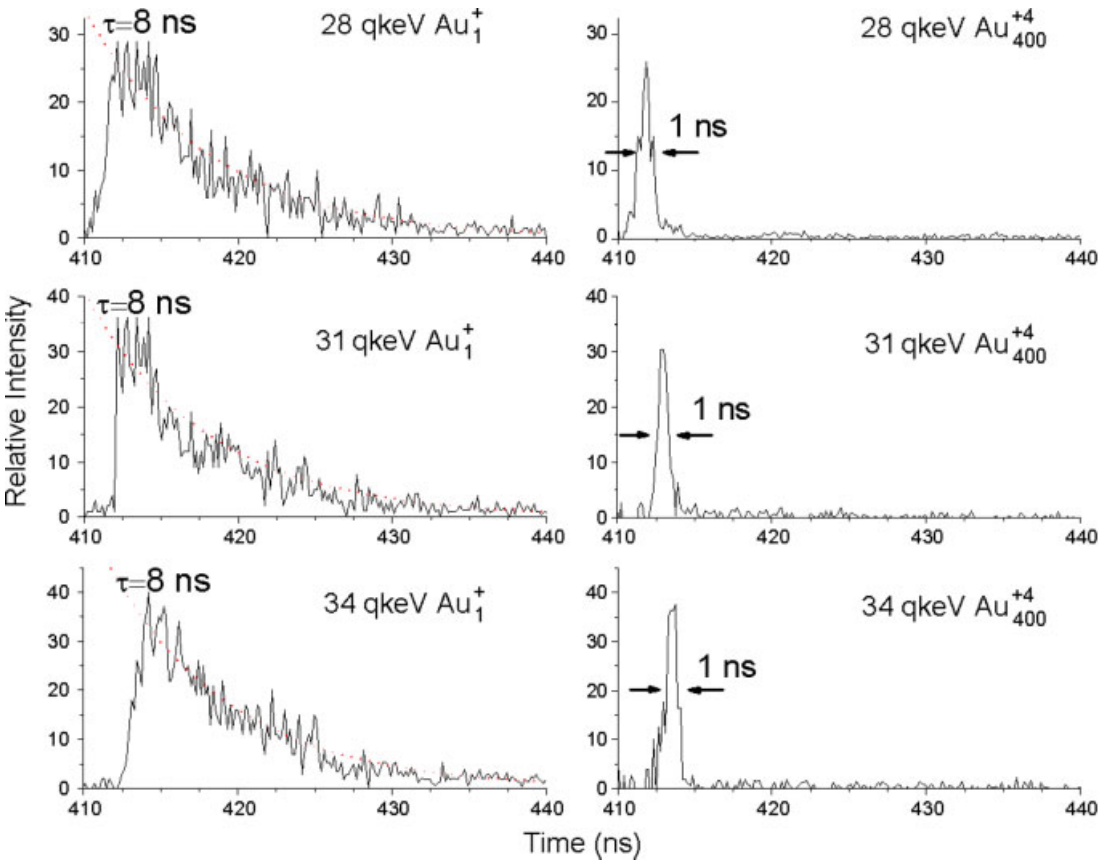

Figure 3. Photon time emission from a CsI/ITO target bombarded with individual gold projectiles as a function of the projectile incident energy (28–34 qkeV). Differences in the start of the photon signals are a consequence of the electron kinetic energies (3, 5 and 9 keV).

to interatomic transition.[16] There is another component with a large decay time higher than 1 μs corresponding to a light emission at 500 nm wavelength which corresponds to probably defects in the crystal. In fact, the fast component is split and two time components observed at room temperature around 6–10 ns and 28–36 ns.[13,17–19] In addition to these two components, a few authors also observed a very fast component with 0.7–2 ns decay time.[14,16,19] Keszthelyi-Lándori *et al*.[16] show clearly that the decay time, the intensity ratio of the two fast components and the presence of the slow component are correlated with the preparation methods. More details on the ratio between the fast emission components can be found in Ref [16]. To our knowledge, we report the first observation of the preeminence of the ultrafast component of the light emission. The use of massive cluster introduces a new process to deposit the energy in the solid and the difference observed with gold atomic ion in this work, and also the results obtained with photons and alpha particles is the consequence of the different ionization density as well as the different path-length. As is indicated by Keszthelyi-Lándori *et al*.,[16] a correlation study between the different fast decay times and the components of the 300 band nm must be performed.

Figure 3 shows the time-resolved photon emission produced during the impact of gold monoatomic (Au_1^+) and massive (Au_{400}^{+4}) projectiles onto a CsI/ITO target as a function of the impact energy (28–34 qKeV). As the impact energy increases a higher number of photons is emitted, while the photon emission distribution profile remains the same. In the energy interval considered here (28–31–34 qKeV), the photon yields increase from 1 to 1.2 to 1.3 for Au_1^+, and from 1 to 1.3 to 1.7 for Au_{400}^{+4}.

Photon and secondary ion emission yields as a function of the 34 qkeV gold projectile size are presented in Fig. 4 for a CsI/ITO target. The secondary ion emission is illustrated in Fig. 4a) for the case of the $(CsI)_nI^-$ cluster ions. For small polyatomic projectiles Au_{1-9}^+, the secondary ion yield (e.g. number of SIs detected per projectile impact) follows a well documented trend.[20] For massive projectiles $Au_{n>9}^{+4}$, the key parameter for secondary ion emission is the energy deposited per unit volume in the solid.[10–12] A different trend is observed in the photon emission from CsI/ITO as a function of the gold projectile size (Fig. 4b)): the number of emitted photons decreases as the projectile size increases from monoatomic to polyatomic projectiles (at the same kinetic energy), while the number of emitted photons increases as the number of constituents increases in the case of the massive gold projectiles. The different behavior observed for the SIs and the photon emission as a function of the projectile size reflects the different modes of interaction between atomic and polyatomic (Au_{1-9}^{+1}) and massive cluster ($Au_{100-400}^{+4}$) projectiles. The decrease in the photon emission as a function of the projectile size for Au_{1-9}^{+1} is related to the decrease in the projectile velocity and excited volume (shorter range and excitation track) as the projectile size increases. For the massive clusters, there is slight increase in the photon emission as a function of the projectile size, *n*. There is evidence the massive projectile interaction proceeds in penetration mode with a high energy density deposited in a small volume.[10,11] Thus, at constant impact energy, the higher the

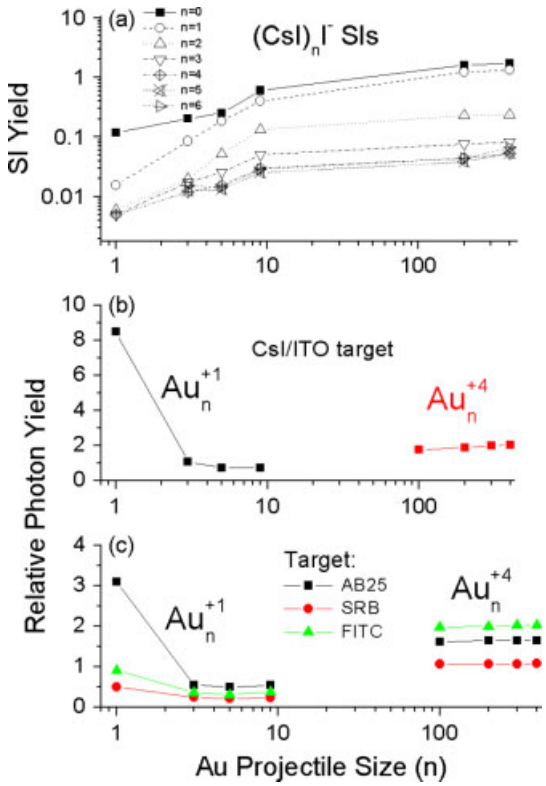

Figure 4. a) Secondary ion, and b) photon yields for a CsI/ITO target as a function of the gold projectile size. c) Photon yields for a series of organic targets: Acid Blue 25 (AB25), Sulforodhamine B (SRB), and Fluorescein isothiocyanate (FITC). All data correspond to 34 qkeV impact energy and relative photon yields have an error of 0.2.

mass, the larger the energy density, with a corresponding trend in photon yield.

It should be pointed out that these measurements were performed at the same impact kinetic energy; however, a sublinear increase in number of photons may be expected for projectiles with the same velocity as the projectile size increases.[7] This last effect will be even more accentuated in the case of the massive gold projectiles. Similar photon yield dependences as a function of the projectile size at the same impact energy (34 qkeV) were observed for a variety of organic targets (Fig. 4c)); we note again, for massive cluster projectiles, a small variation in the number of emitted photons with the number of projectile constituents.

Coincidence measurements of photon, electron and negative SIs were performed as a function of the projectile size and impact energy (schematic of setup in Fig. 1). In the case of massive projectiles ($Au_{100-400}^{+4}$), the concurrent emission of photons, electrons and negative SIs was observed for individual projectile impacts. Preliminary results show that electron emission for massive gold projectiles occurs under unlikely conditions well below the classical kinetic emission threshold,[21,22] e.g. electron emission was observed for massive projectiles ($Au_{100-400}^{+4}$) with impact energies as low as ~190 eV/atom. While the number of electrons emitted depends on the nature of the target, electron emission was observed from both inorganic and organic targets. As noted earlier, we interpret the electron emission from massive projectile impacts to be the consequence of electronic excitation via a collective effect, which remains to be elucidated.

Conclusion

The concurrent emission of photons, electron and negative SIs from projectile-solid interactions in the hydrodynamic mode are reported for the first time. The mechanisms coupling the projectile energy into atomic and molecular electronic excitation remain to be elucidated. Photon yield data for a wide range of projectile-target characteristics are a prerequisite for progress in the understanding of the fundamental aspects. From one applied perspective, the relevance of studying photon emission from nanoparticle hydrodynamic penetration may be derived from the trends observed in discrete hypervelocity microparticle impacts: '... the maximum light intensity and the total light energy are unique functions of the mass and velocity of the impacting projectile'.[9] In the case considered here, the projectile parameters are known; variations in photon emission will reflect target characteristics. Thus, we expect a trend in photon emission where larger momentum impacts than those used here will boost an already notable photon yield to the level of a useful complimentary signal to ion emission for surface characterization.

Acknowledgments

This work was supported by the National Science Foundation (Grant CHE-0750377) and the Robert A. Welch Foundation (Grant A-1482).

References

[1] J. S. Colligon, *Vacuum* **1974**, *24*, 373.
[2] N. H. Tolk, I. S. T. Tsong, C. W. White, *Anal. Chem.* **1977**, *49*, 16A.
[3] C. W. White, D. L. Simms, N. H. Tolk, *Science* **1972**, *177*, 481.
[4] G. M. McCracken, S. K. Erents, *Phys. Lett. A* **1970**, *31*, 429.
[5] M. Zivitz, E. W. Thomas, *Nucl. Instrum. Methods* **1976**, *132*, 411.
[6] R. G. Kaercher, E. F. da Silveira, J. F. Blankenship, E. A. Schweikert, *Phys. Rev. B* **1995**, *51*, 7373.
[7] K. Baudin, E. S. Parilis, J. F. Blankenship, M. J. Van Stipdonk, E. A. Schweikert, *Nucl. Instrum. Methods Phys. Res. Sect. B* **1998**, *134*, 352.
[8] R. E. Johnson, B. U. R. Sundqvist, W. Ens, *Rapid Commun. Mass Spectrom.* **1991**, *5*, 574.
[9] G. Eichhorn, *Planet. Space Sci.* **1976**, *24*, 771.
[10] T. J. Colla, H. M. Urbassek, *Nucl. Instrum. Methods Phys. Res. Sect. B* **2000**, *164–165*, 687.
[11] C. Guillermier, S. Della-Negra, E. A. Schweikert, A. Dunlop, G. Rizza, *Int. J. Mass Spectrom.* **2008**, *275*, 86.
[12] S. Bouneau, S. Della-Negra, J. Depauw, D. Jacquet, Y. Le Beyec, J. P. Mouffron, A. Novikov, M. Pautrat, *Nucl. Instrum. Methods Phys. Res. Sect. B* **2004**, *225*, 579.
[13] S. Kubota, S. Sakuragi, S. Hashimoto, J-z. Ruan, *Nucl. Instrum. Methods Phys. Res. Sect. A* **1988**, *268*, 275.
[14] P. Schotanus, R. Kamermans, *IEEE Trans. Nucl. Sci.* **1990**, *37*, 177.
[15] J. Pouthas, B. Borderie, R. Dayras, E. Plagnol, M. F. Rivet, F. Saint-Laurent, J. C. Steckmeyer, G. Auger, C. O. Bacri, S. Barbey, A. Barbier, A. Benkirane, J. Benlliure, B. Berthier, E. Bougamont, P. Bourgault, P. Box, R. Bzyl, B. Cahan, Y. Cassagnou, D. Charlet, J. L. Charvet, A. Chbihi, T. Clerc, N. Copinet, D. Cussol, M. Engrand, J. M. Gautier, Y. Huguet, O. Jouniaux, J. L. Laville, P. Le Botlan, A. Leconte, R. Legrain, P. Lelong, M. Le Guay, L. Martina, C. Mazur, P. Mosrin, L. Olivier, J. P. Passerieux, S. Pierre, B. Piquet, E. Plaige, E. C. Pollacco, B. Raine, A. Richard, J. Ropert, C. Spitaels, L. Stab, D. Sznajderman, L. Tassan-got, J. Tillier, M. Tripon, P. Vallerand, C. Volant, P. Volkov, J. P. Wieleczko, G. Wittwer, *Nucl. Instrum. Methods Phys. Res. Sect. A* **1995**, *357*, 418.
[16] S. Keszthelyi-Lándori, I. Földvári, R. Voszka, Z. Fodor, Z. Seres, *Nucl. Instrum. Methods Phys. Res. Sect. A* **1991**, *303*, 374.
[17] C. L. Woody, P. W. Levy, J. A. Kierstead, T. Skwarnicki, Z. Sobolewski, M. Goldberg, N. Horwitz, P. Souder, D. F. Anderson, *IEEE Transactions Nucl. Sci.* **1990**, *37*, 492.

[18] C. Amsler, D. Grögler, W. Joffrain, D. Lindelöf, M. Marchesotti, P. Niederberger, H. Pruys, C. Regenfus, P. Riedler, A. Rotondi, *Nucl. Instrum. Methods Phys. Res. Sect. A* **2002**, *480*, 494.
[19] A. N. Belsky, A. N. Vasil'ev, V. V. Mikhailin, A. V. Gektin, N. V. Shiran, A. L. Rogalev, E. I. Zinin, *AIP* **1992**, 806.
[20] M. Benguerba, A. Brunelle, S. Della-Negra, J. Depauw, H. Joret, Y. Le Beyec, M. G. Blain, E. A. Schweikert, G. B. Assayag, P. Sudraud, *Nucl. Instrum. Methods Phys. Res. Sect. B* **1991**, *62*, 8.
[21] A. Brunelle, P. Chaurand, S. Della-Negra, Y. Le Beyec, E. Parilis, *Rapid Commun. Mass Spectrom.* **1997**, *11*, 353.
[22] K. Toglhofer, F. Aumayr, H. Kurz, H. Winter, P. Scheier, T. D. Mark, *Europhys. Lett.* **1993**, *22*, 597.